Supplementary Information

Water Splitting with Cobalt-incorporated Ruthenium Sulfide (Co_xRuS) and Molecular Cobalt Porphyrin

Nasim Jafari, Neidy Ocuane, Brenda Torres, Jose L. Lasso, Carlos R. Cabrera, Dino Villagrán*

Corresponding author: Dino Villagrán*

dino@utep.edu

Table of contents

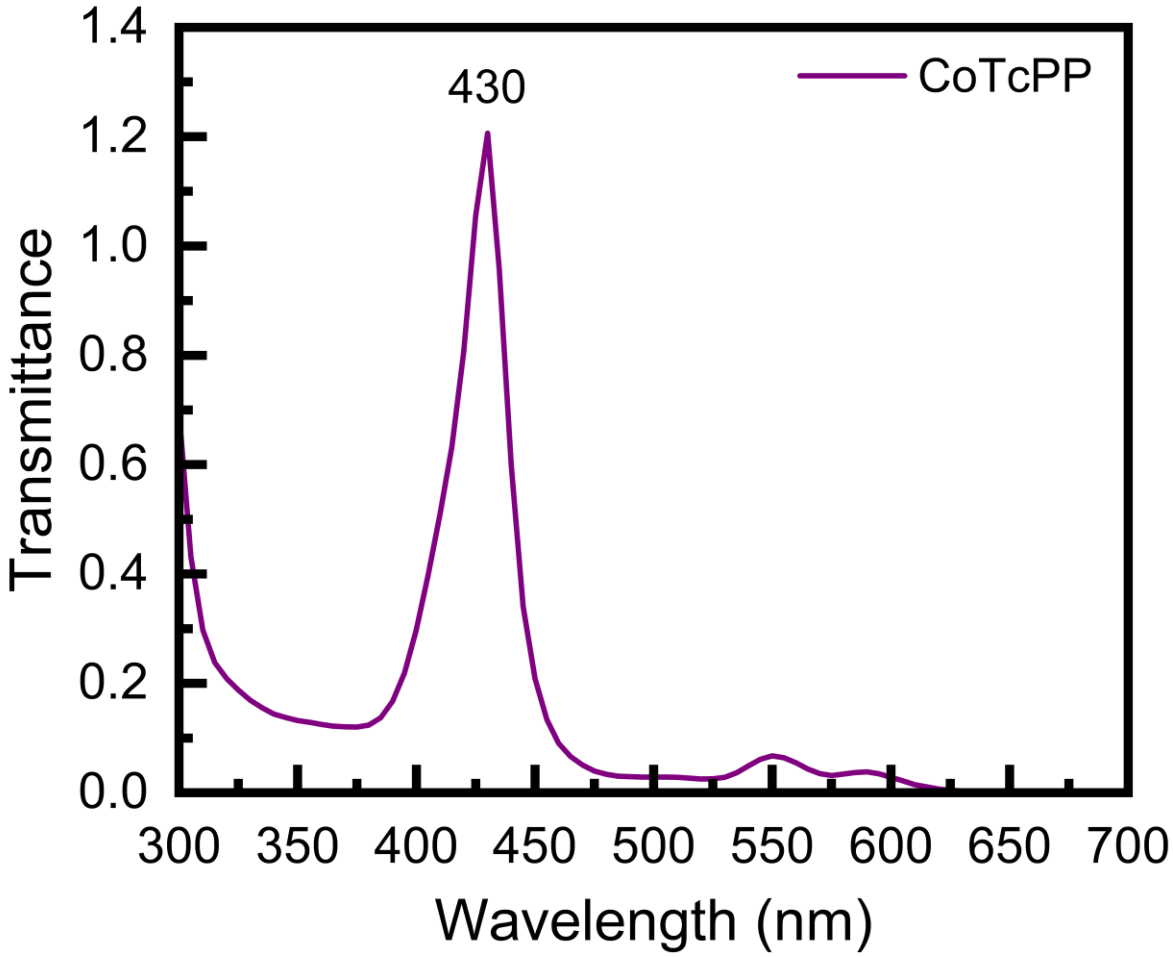

Figure S1. UV-Vis absorption spectrum of CoTcPP, showing a strong Soret band at 430 nm and Q bands of 550 nm and 595 nm, confirming the successful synthesis of CoTcPP.

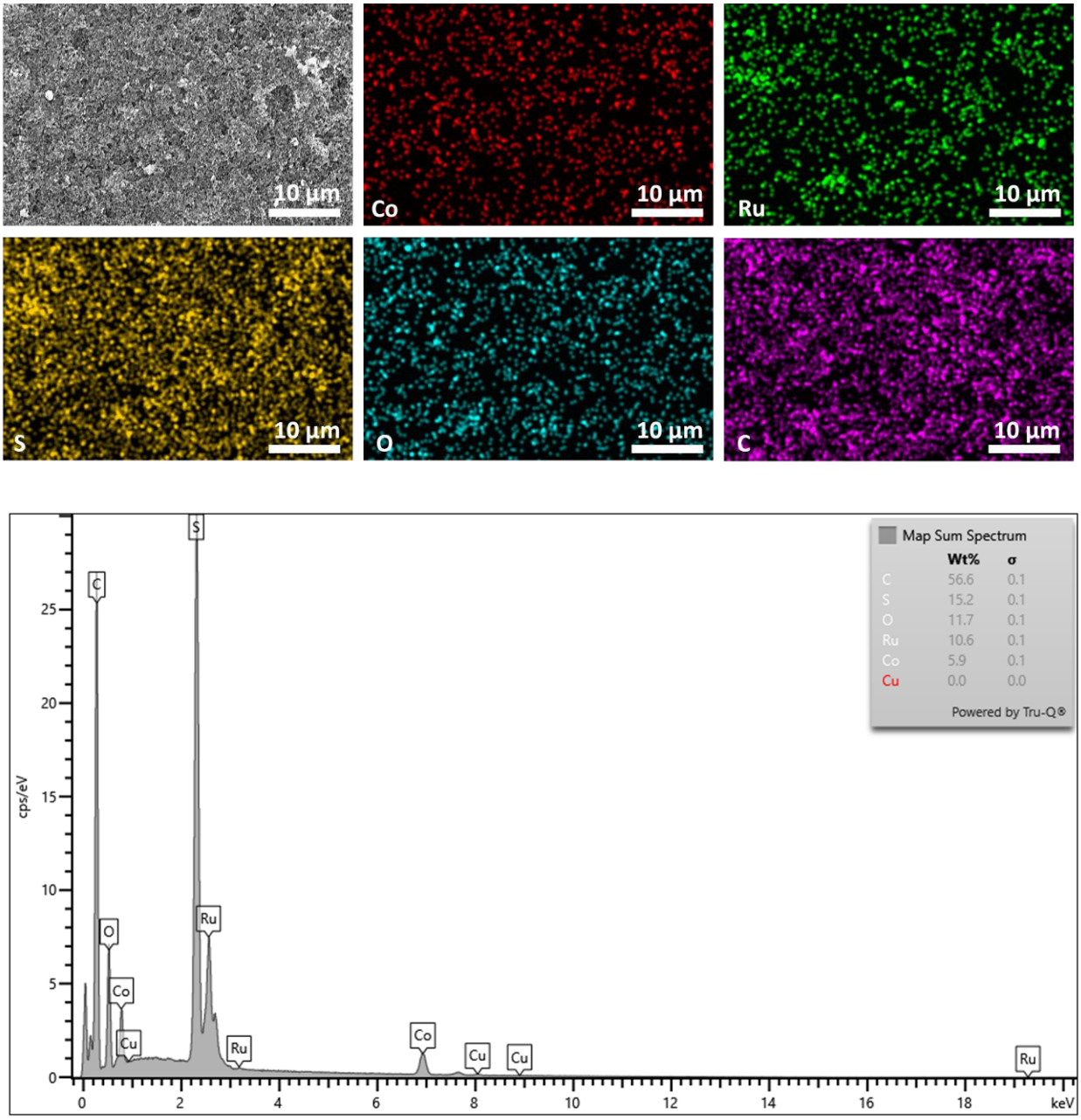

Figure S2. EDS elemental mapping and spectra of the C-Co_4RuS catalyst, showing the uniform distribution of C, Ru, Co, and S elements across the surface of electrode. The detected oxygen likely is from partial surface oxidation of the sulfide, forming oxides or hydroxides during exposure to air.

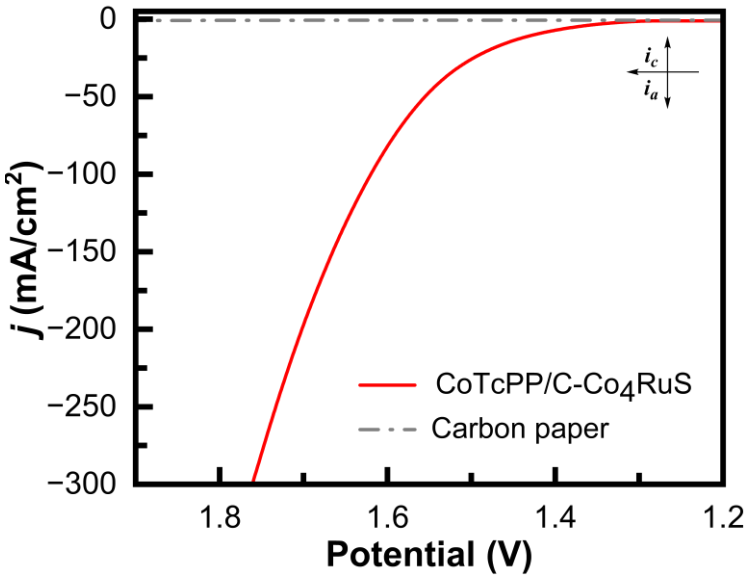

Figure S3. Overall water splitting using CoTcPP/C-Co_4RuS as the OER working electrode and C-Co_4RuS as the HER counter electrode in 1.0 M KOH. As illustrated, the modified electrode system exhibited improved electrocatalytic behavior.

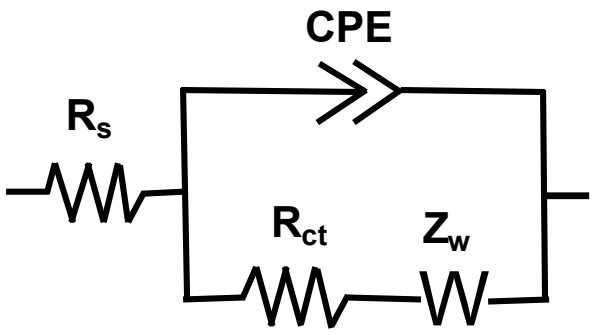

Figure S4. Equivalent circuit model used for EIS fitting, consisting of solution resistance (R_s), charge transfer resistance (R_{ct}), constant phase element (CPE), and Warburg impedance (W) for diffusion processes.

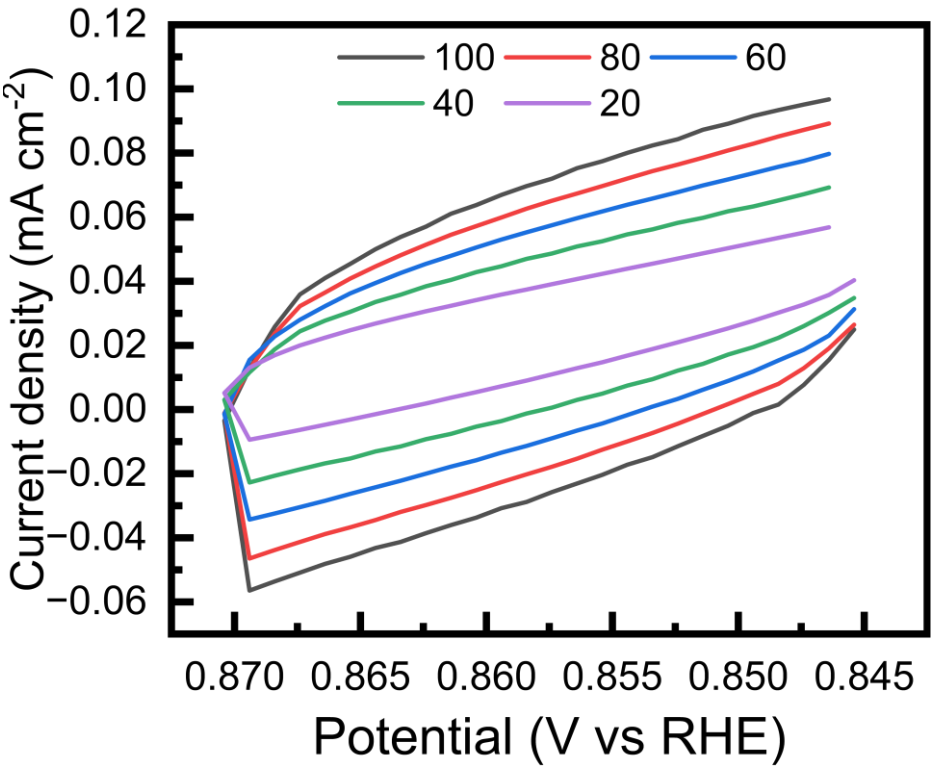

Figure S5. Cyclic voltammograms of C-Co_4RuS recorded in the non-Faradaic potential region at different scan rates (20-100 mV s^{-1}) in 1.0 M KOH. The capacitive current response increases linearly with the scan rate and resulting C_{dl} was 397.2 µF cm^{-2}.

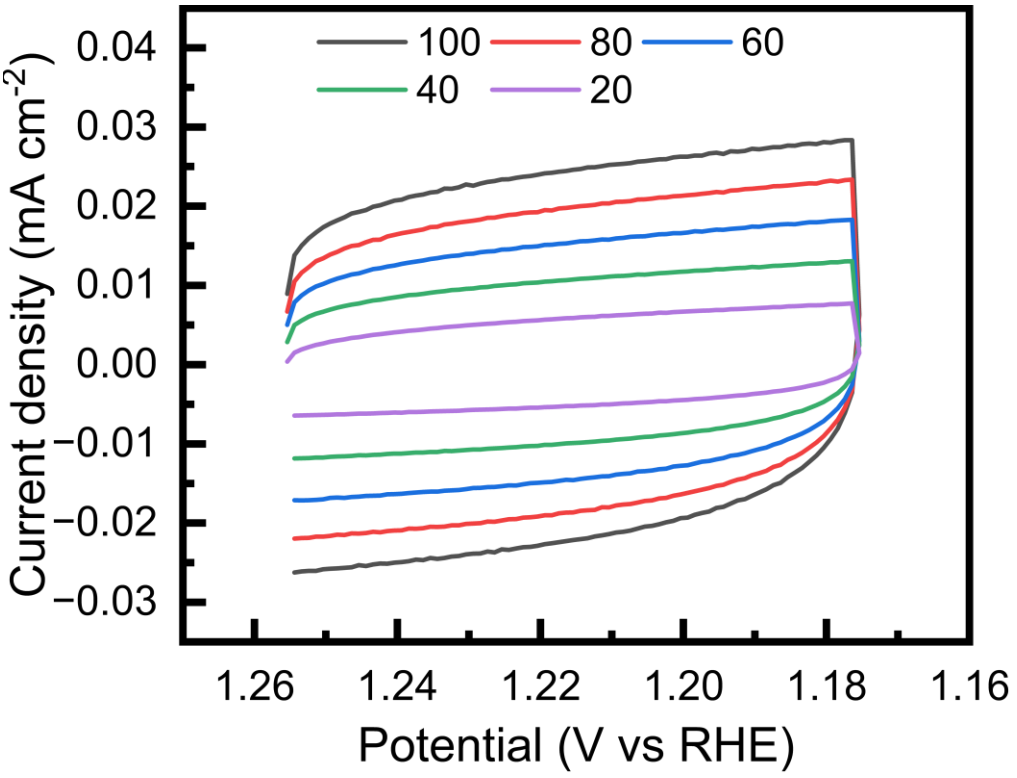

Figure S6. Cyclic voltammograms of CoTcPP recorded in the non-Faradaic potential region at different scan rates (20-100 mV s^{-1}) in 1.0 M KOH. The capacitive current response increases linearly with the scan rate and resulting C_{dl} was 221.6 µF cm^{-2}.

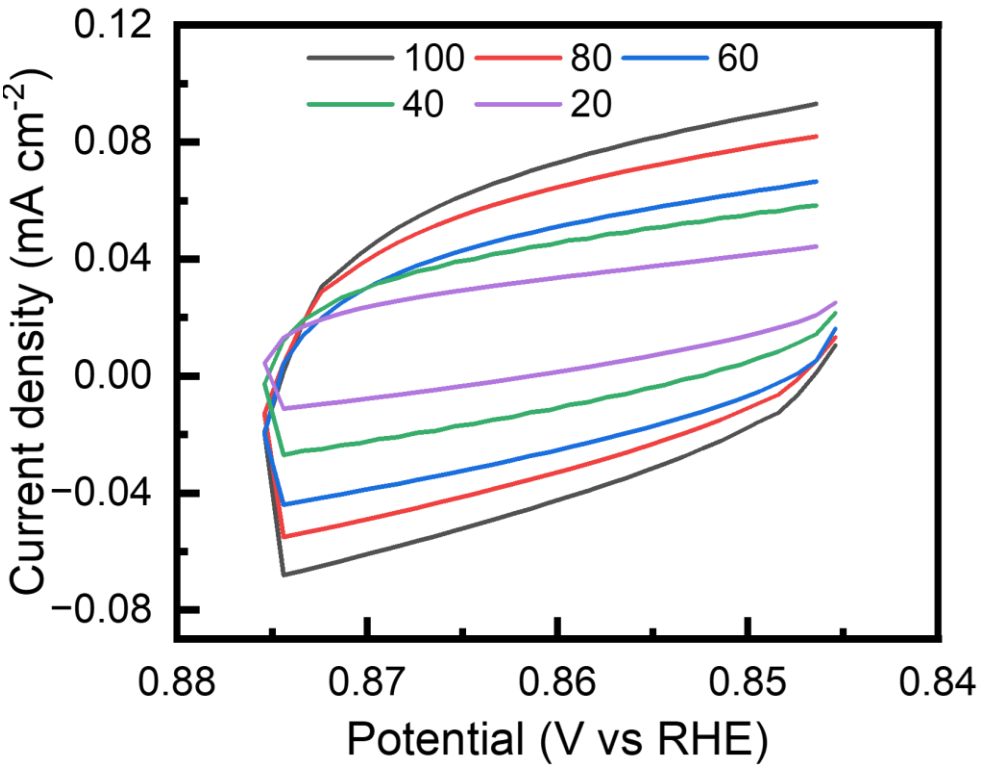

Figure S7. Cyclic voltammograms of CoTcPP/C-Co_4RuS recorded in the non-Faradaic potential region at different scan rates (20-100 mV s^{-1}) in 1.0 M KOH. The capacitive current response increases linearly with scan rate and resulting C_{dl} was 485.1 µF cm^{-2}.

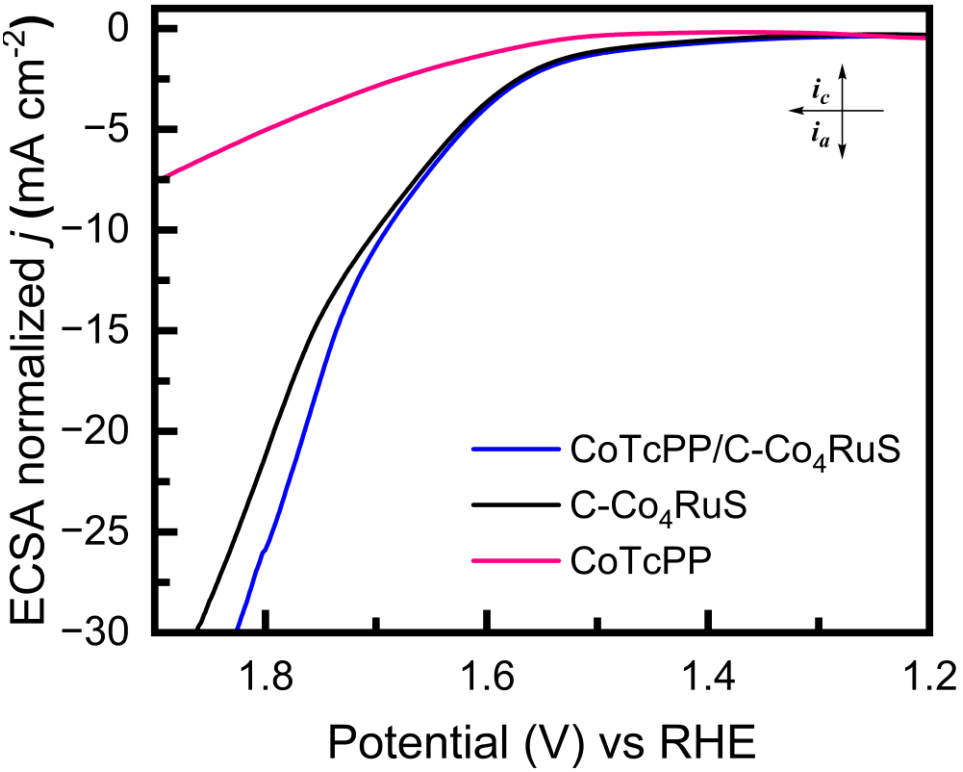

Figure S8. ECSA-normalized OER polarization curves of C-Co_4RuS, CoTcPP, and CoTcPP/C-Co_4RuS in 1.0 M KOH. Current densities were normalized using the estimated electrochemical surface areas obtained by double-layer capacitance (C_{dl}) measurements (CoTcPP: 5.54 cm^2, C-Co_4RuS: 9.93 cm^2, CoTcPP/C-Co_4RuS: 12.13 cm^2).

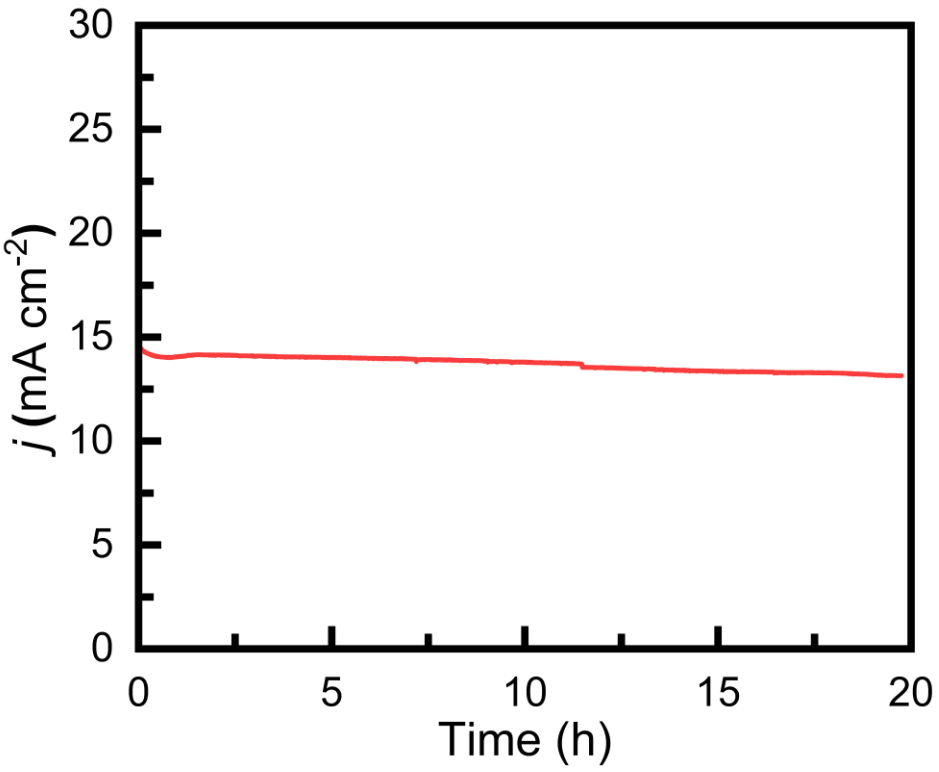

Figure S9. Potentiostatic stability (bulk electrolysis) test of C-Co_4RuS for the hydrogen evolution reaction (HER) at -0.14 V vs RHE in 0.5 M H_2SO_4. The current density only decreases by ~8% over 20 h, which shows the durability of the catalyst under reductive conditions.

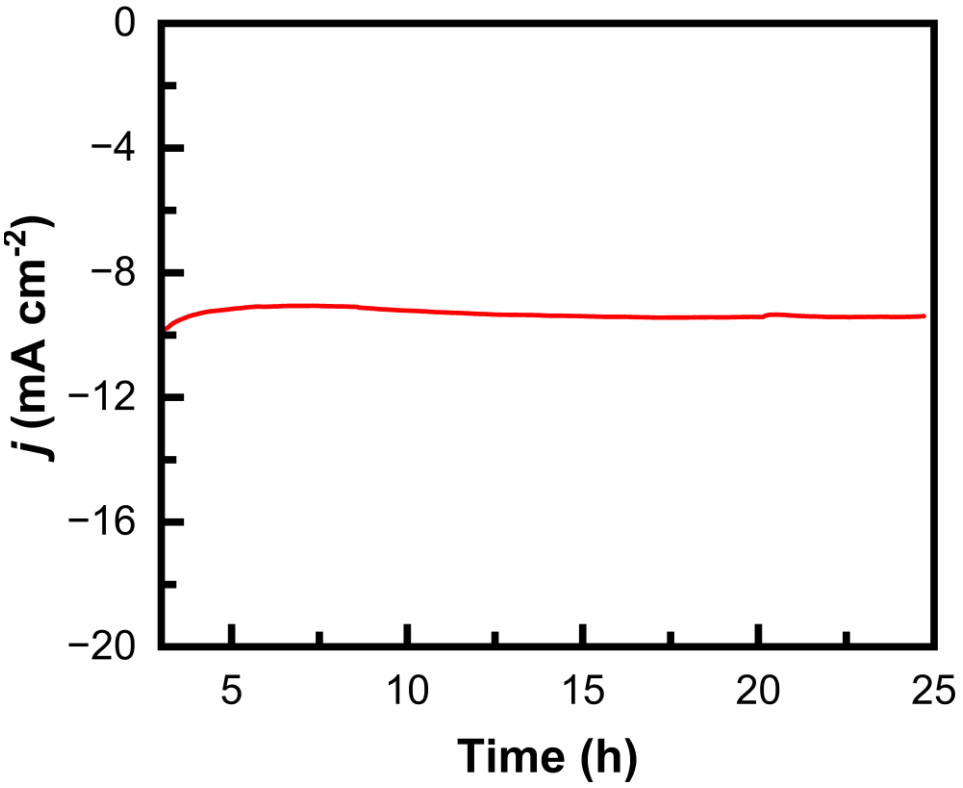

Figure S10. Potentiostatic stability (bulk electrolysis) test of CoTcPP/C-Co_4RuS for the oxygen evolution reaction (OER) at 1.52 V vs RHE in 1.0 M KOH. The current density only decreases by ~3% over 25 h, which shows the durability of the catalyst under oxidative conditions.

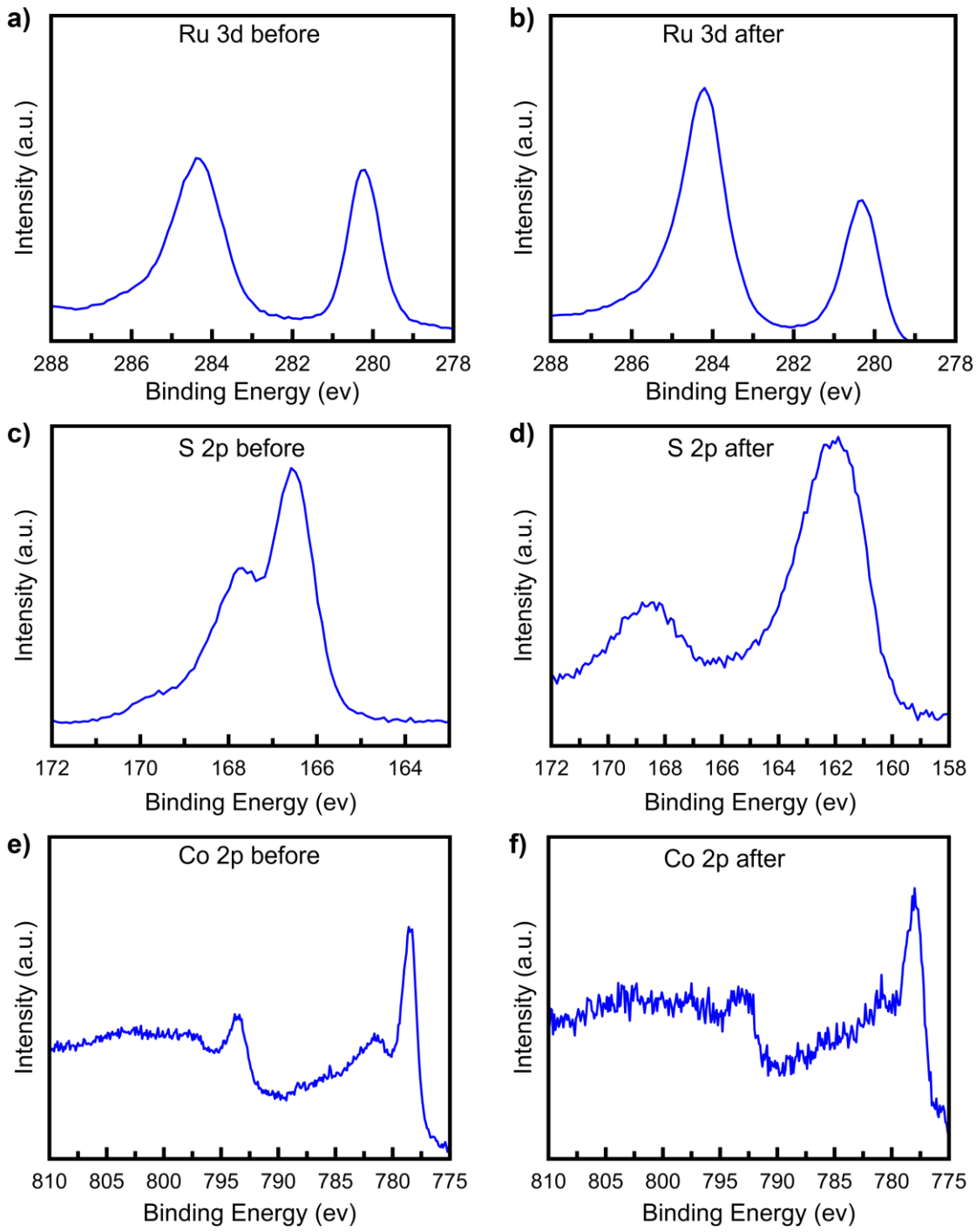

Figure S11. XPS spectra of CoTcPP/C-Co_4RuS before and after 25 h bulk electrolysis in oxidation condition. The comparison shows that the main elemental signals remain present after the stability test, confirming the overall retention of the catalyst composition. At the same time, changes in peak profile and relative intensity are observed after electrolysis, indicating surface chemical evolution, including partial oxidation (Such as surface oxidized sulfur species) and reconstruction under operating conditions.

Table S1. Estimated nominal Ru loading of catalyst-coated electrodes and corresponding OER overpotential at 10 mA cm^{-2} in KOH 1M.

Catalyst	η_{10} (mV)	Ru Loading (μg cm^{-2})
C-RuS	379	~35.1–36.7
C-CoRuS	265	~22.1–23.4
C-Co_2RuS	283	~15.0–15.9
C-Co_4RuS	257	~9.2–9.8
CoTcPP/C-Co_4RuS	202	~8.3–8.8

Table S2. Fitted electrochemical impedance spectroscopy (EIS) parameters for bare carbon paper, C-RuS, C-Co_4RuS, CoTcPP, and the CoTcPP/C-Co_4RuS composite, based on the equivalent circuit model. R_s represents the solution resistance, R_{ct} is the charge transfer resistance, CPE is the constant phase element with its corresponding exponent *n*, and W is the Warburg impedance reflecting diffusion processes. The CoTcPP/C-Co_4RuS composite exhibits the lowest R_{ct} and acceptable X^2 value, indicating a better charge-transfer efficiency than other samples.

Equivalent circuit parameters	Carbon paper	C-RuS	C-Co_4RuS	CoTcPP	CoTcPP/C-Co_4RuS
R_s	19.01	25.07	4.802	15.93	12.92
CPE	3.70E-06	1.55E-03	2.86E-03	2.10E-03	3.64E-03
n	0.9009	0.5163	0.2394	0.5716	0.3518
R_{ct}	1495	183.7	18.10	35.39	12.79
W	80.59	74.52	118.1	46.54	139.6
X^2	0.02826	0.01867	0.01970	0.01021	0.02096

Table S3. Comparison of the oxygen evolution reaction (OER) activity of CoTcPP/C-Co_4RuS with representative Ru-based electrocatalysts reported in alkaline media. The overpotential required to reach 10 mA cm^{-2} (η_{10}) is listed together with the Ru loading information as reported in the original literature. Where direct areal Ru loading values were not explicitly provided, the reported Ru content or estimated nominal loading is shown. Because catalyst preparation methods, substrates, and loading descriptors differ among studies, the comparison is intended to provide performance context rather than a strict one-to-one ranking.

Catalyst	Electrolyte	η10 for OER (mV)	Ru loading information
CoTcPP/C-Co_4RuS (this work)	1.0 M KOH	202	Nominal 8.3–8.8 μg Ru cm^{-2}
Ru/CoFe-LDH [1]	1.0 M KOH	198	0.45 wt% Ru
$Ru_{0.9}Co_{0.1}O_y$ [2]	1.0 M KOH	290	Not explicitly reported, mass activity calculated from thin-film mass
Ru–$Ni(OH)_2$ [3]	1.0 M KOH	231.9	Ru mass fraction in electrode = 0.51 wt%, actual Ru/Ni molar ratio ≈ 0.35%
Ru-SAC/$NiCo_2O_4$ [4]	1.0 M KOH	280 (1.51 V vs RHE at 10 mA cm^{-2})	2.03 wt% Ru, catalyst loading 0.25 mg on 0.16 cm^2, giving an estimated 31.7 μg Ru cm^{-2}
Ru–O–Mn/CPD [5]	1.0 M KOH	194	Estimated areal Ru loading ≈ 211 μg cm^{-2} (from 41.4 wt% Ru and electrode ink deposition)
RuNiOx [6]	1.0 M KOH	210	Ru loading not explicitly reported, prepared by dip-coating from 5 mmol $RuCl_3$ + 5 mmol Ni precursor solution onto 1 × 2 cm Ti foam

References:

1 P. Li, M. Wang, X. Duan, L. Zheng, X. Cheng, Y. Zhang, Y. Kuang, Y. Li, Q. Ma, Z. Feng, W. Liu and X. Sun, *Nat Commun*, 2019, **10**, 1711.

2 M. M. Tellez-Cruz, A. Serrano-Lázaro, L. I. Olvera and M. Bizarro, *International Journal of Hydrogen Energy*, 2025, **168**, 150964.

3 J. Qi, R. Xu, T. Yang, M. Yang, J. Chen, J. Tu, B. Wang, C. Qu, Z. Wang, J. Cao and Y. Yan, *J. Mater. Chem. A*, 2025, **13**, 26555–26563.

4 A. Gupta, S. Ghosh, D. Bhalothia, S. Thangarasu, B. Ghosh, R. Urkude, J. Chowdhury and S. Pande, *J. Mater. Chem. A*, 2024, **12**, 23819–23836.

5 T. Feng, J. Yu, D. Yue, H. Song, S. Tao, G. I. N. Waterhouse, S. Lu and B. Yang, *Applied Catalysis B: Environmental*, 2023, **328**, 122546.

6 Y.-J. Ko, M. H. Han, C. Lim, S.-H. Yu, C. H. Choi, B. K. Min, J.-Y. Choi, W. H. Lee and H.-S. Oh, *Journal of Energy Chemistry*, 2023, **77**, 54–61.